Microsystem Technologies (2019) 25:3923–3932
https://doi.org/10.1007/s00542-019-04380-9

TECHNICAL PAPER

Gas-assisted thermal bonding of thermoplastics for the fabrication of microfluidic devices

S. R. Mahmoodi[1] · P.-K. Sun[2] · M. Mayer[2] · R. S. Besser[2]

Received: 19 November 2018 / Accepted: 28 February 2019 / Published online: 18 March 2019

Abstract
The challenges for high-strength adhesive-free sealing of thermoplastic microfluidics have impeded commercialization. We present the technique of gas-assisted thermal bonding (GATB) for joining thermoplastic surfaces at elevated temperatures to produce microfluidic devices with low distortion. In this technique a pressurized gas is used to supply the force to bond the two substrates rather than relying on direct contact of thermoplastics with a rigid press. Mechanical characterization tests were performed to analyze and optimize the effect of GATB pressure and temperature on the bonding strength of laminated polymethyl-methacrylate (PMMA) membranes. Tensile tests on PMMA membranes subjected to GATB process conditions examined the effects of these conditions on the single membrane's characteristics. Adhesive strength was assessed on thin PMMA strips bonded together by GATB in lap shear and T-peel test configurations. The maximum lap shear and peel strength were found to occur at the lowest tested pressure of 1.17 MPa based on bonding experiments at 160 °C and 180 °C, respectively. Thereafter, the GATB is compared with the conventional plate-to-plate method to bond a capping sheet on pre-fabricated microchannels. Channel deformation is quantified by cross-section imaging before and after the sealing experiments. It was found that GATB enables low-distortion microchannels with higher uniformity at elevated temperatures, providing a solution for adhesive-free manufacturing of thermoplastic-based microfluidic systems.

1 Introduction

Microfluidic devices have shown considerable promise in a wide range of applications from medical screening to portable energy sources (McDonald and Whitesides 2002; Guber et al. 2004). For many of these devices the critical barriers to be resolved before commercialization are cost-effective manufacturing and high performance (Chin et al. 2012; Sackmann et al. 2014). The limitations of conventional silicon- or glass-based processing techniques have prompted researchers to explore alternative materials (Narasimhan and Papautsky 2003). Initially, PDMS was viewed as a logical base material (Berthier et al. 2012). However, in recent years, there has been a tendency towards the employment of thermoplastics for microfluidic systems due to material property issues associated with PDMS, such as surface treatment instability, bulk absorption of small molecules and evaporation through the device (Sackmann et al. 2014; Miserere et al. 2012). Thermoplastic polymers offer a number of advantages, which include a wide range of physical and chemical properties, biochemical compatibility, ease of processing and prototyping, light-weight and low cost (Narasimhan and Papautsky 2003; Tsao et al. 2007). As a result, thermoplastic microfluidic systems based on PMMA, polycarbonate (PC), cyclic olefin polymers (COP) or copolymers (COC) have gained increasing attention. Although COC and COP have recently presented as highly attractive candidates, the use of PC and PMMA in microfluidic studies is favorable due to the many advantages like wide availability in a variety of grades, good chemical compatibility, and molding properties (Tsao and DeVoe 2009).

Injection molding, hot embossing, casting and laser micro-machining are the common techniques that have been used for polymer-based microfabrication (Becker and Gärtner 2008; Becker and Locascio 2002; Su et al. 2003).

✉ S. R. Mahmoodi
reza.mahmoodi@rutgers.edu

[1] Department of Electrical and Computer Engineering, Rutgers University, 94 Brett Rd, Piscataway, NJ 08854, USA

[2] Department of Chemical Engineering and Materials Science, Stevens Institute of Technology, Castle Point on Hudson, Hoboken, NJ 07030, USA

Thermoplastic polymers are the most suitable materials for scaling up in a production process through established techniques like embossing or injection molding (Marasso et al. 2014). Among these fabrication methods, CO_2 laser micromachining offers rapid prototyping and iterative design of microfluidic devices, proven to be an effective technique for scientific trials and small-scale production (Matellan and Armando 2018). Regardless of the fabrication method employed, one of the key challenges in creating most microfluidic devices is to seal a cap on a substrate containing microscale channels. As a result, bonding of two or more parts is a fundamental issue for nearly all microfluidic devices (Tsao and DeVoe 2009).

In direct thermal bonding, substrates are normally heated to a temperature near or above the glass transition temperature (T_g) of one or both substrate materials, while simultaneously applying pressure. Optimization of the bonding parameters (temperature, pressure and time) is crucial for successful sealing and has been the subject of many studies (Eddings et al. 2008; Brown et al. 2006; Zhu et al. 2007). The use of inappropriate parameter settings can result in microstructure deformation and collapse. Alternatively, techniques like solvent and adhesive bonding have been used to reduce the required bonding temperature (Velten et al. 2005; Park et al. 2012; Brown et al. 2006), giving more flexibility in the selection of materials for the components (Carlborg et al. 2011; Folch 2016). However, these methods result in inhomogeneous sidewalls and the challenge of microchannel clogging becomes a major issue (Tsao and DeVoe 2009; Ogilvie et al. 2010).

Different fabrication methods to generate complete Lab-on-a-Chip solutions based on thin and flexible films (Lab-on-a-Foil) have been previously reviewed by Focke et al. (2010). In a second review paper (Truckenmüller et al. 2011), thermoforming of film-based biomedical microdevices was explored. In addition, fabrication techniques like micro pressure forming (Truckenmüller et al. 2011), vacuum bagging (Cassano et al. 2015), thermal bonding in water (Kelly and Woolley 2003), gas-assisted embossing (Peng et al. 2014), UV-nanoimprint lithography (Chen et al. 2015), pressure sensitive film sealing (Huang et al. 2007), interfacial layer bonding (Chow et al. 2005), roll-to-roll lamination (Miserere et al. 2012), and rubber-assisted hot embossing (Nagarajan and Yao 2011) have been previously introduced and studied. However, to the authors' knowledge, bonding of polymer-based substrates have not been investigated by an air-cushion press (ACP). The present study adds a new approach to this list for cost-effective fabrication of polymer-based devices, capable of targeting various applications for low-cost and light-weight disposable chips.

ACP technology has formerly been employed to advance hot embossing technology (Guo 2007). In a hot embossing process equipped with ACP, called gas-assisted hot embossing (Peng et al. 2014), a pressurized fluid presses a solid mold and substrate against one another to stamp the intermediate layer, with improved pressure uniformity, yield, and stamping speed (Gao et al. 2006). In this work, the ACP technology commonly used in hot embossing has been adapted to bond polymer substrates together as an advancement to the common plate-to-plate method used in thermoplastic-based microfluidic sealing. Figure 1 illustrates the GATB in comparison with plate-to-plate thermal bonding.

In the present work, GATB process parameters are studied by measuring the bonding strength between PMMA surfaces. The bonding strength is quantitatively represented by the lap shear failure load and peeling strength. As a point of reference, the characteristic PMMA tensile strength was determined both for untreated samples and for samples treated under GATB bonding conditions to quantify the effect of processing and to contrast with the bonding strength results. Finally, the GATB method is compared with the conventional plate-to-plate hot pressing to bond a capping on pre-fabricated microchannels. Microchannel deformation in both cases is estimated by cross-section imaging before and after the sealing process at elevated temperatures.

2 Experimental

0.05-mm-thick PMMA strips (Goodfellow Corp.) were used as the bonding materials for mechanical testing. For the mechanical strength measurements, the PMMA thin strips were cut along their long dimension as received. Figure 2a–c illustrates the three different mechanical tests performed on the flexible PMMA films. First, tensile tests were done on single layer unbonded strips exposed to the GATB conditions to understand the effect of the process parameters on the characteristics of PMMA film. For this reason, rectangular test specimens (20 mm length and 10 mm width) were prepared and then tested at both untreated and after experiencing various GATB treatment conditions. GATB treatment was performed on a batch of single samples at a constant pressure of 1.38 MPa at five different temperatures ranging from 140 to 180 °C in 10 °C increments.

Lap shear and T-peel experiments were used to quantify and compare the failure strength of the bonded samples. The T-peel specimens were bonded by the GATB method at three different pressures of 1.17 MPa, 1.38 MPa, and 1.59 MPa, and temperatures from 140 to 180 °C. The lap shear specimens were prepared at the same pressures but

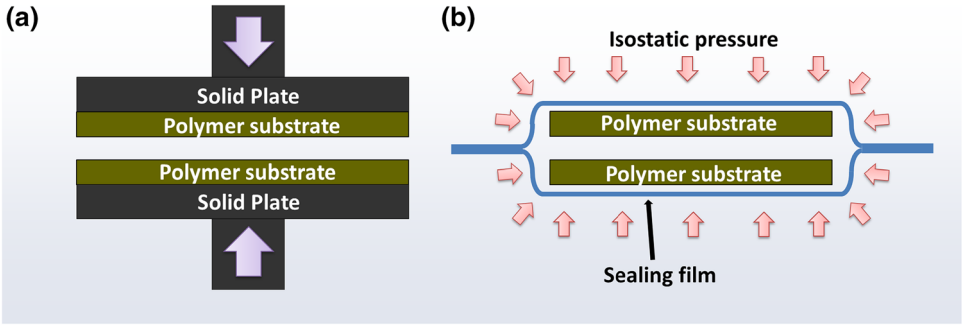

Fig. 1 Conceptual representation of comparison between **a** plate-to-plate thermal bonding, and **b** GATB techniques

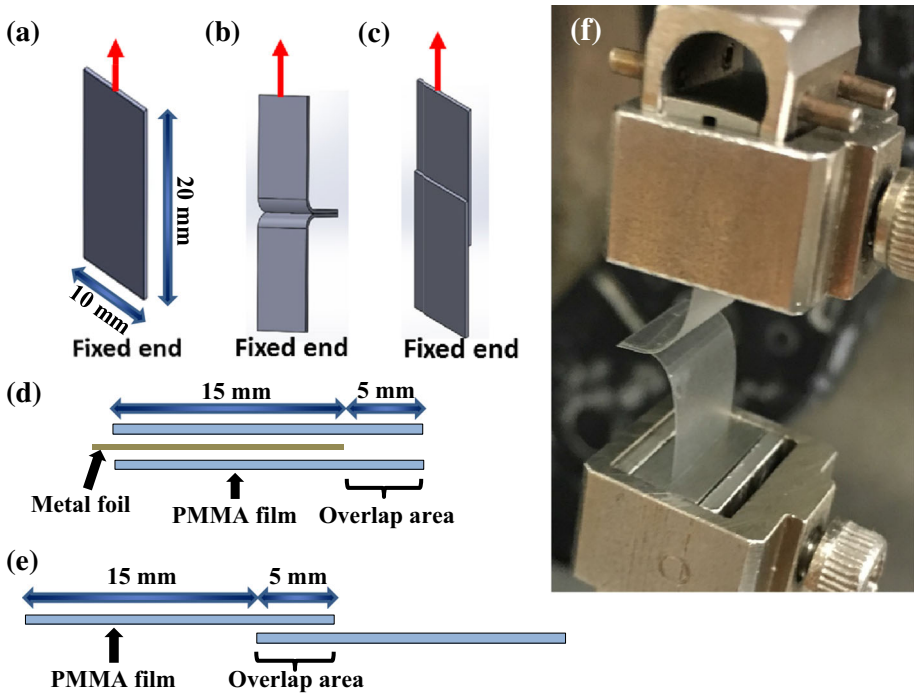

Fig. 2 3D scheme of **a** tensile test, **b** T-peel test, and **c** lap-shear test. Illustration of bonding arrangement in **d** T-peel test, and **e** single lap-shear test. **f** Experimental setup used for the T-peel test

with bonding temperatures from 130 to 180 °C in 10 °C increments. For the lap shear and T-peel sample preparation, two thin strips of PMMA with an overlap area of 5×10 mm^2 were laminated as shown in Fig. 2d, e. As illustrated, single lap shear and T-peel specimens were prepared from two PMMA films that overlap in the joint area. PMMA films were bonded without any prior surface treatment and remained under bonding conditions for 1 min. The unbonded area of the T-peel strips were created by interposing a removable metal foil between the laminating layers. At least three samples were tested under identical conditions to ensure the reproducibility of the results. All mechanical tests were measured with a rheometer (Fig. 2f) equipped with a 2 kgf load cell (Rheometric Scientific, ARES RDA-II) for tensile testing at room temperature. The grip-to-grip distance was set to be 1.6 cm and the samples were loaded at a speed of 0.1 mm/s in all mechanical tests.

The GATB process employs a nanoimprint lithography (NIL) apparatus (Nanonex, NX-1000) originally dedicated to thermal NIL (Tan et al. 2004; Zhou 2013). Figure 3 illustrates the apparatus utilized for bonding the polymer components. The gas pressure is transferred to the sample, which is sandwiched between two sealing films. Prior to the introduction of the pressurized nitrogen gas into the chamber, the sealing films and the sample are put into contact under vacuum. During the process, the temperature over the components is precisely controlled by an IR-lamp and a thermocouple near the sample. The diameter of the sample processing area is 110 mm, which provides enough area to press a batch of five bonding specimens in our experiments. The tool is capable of GATB processing (with a dwell time of 1 min) of about twelve batches per hour.

For proof of concept, the GATB technique was used to seal microfluidic channels. 2-mm-thick PMMA acrylic sheets (ePlastics Corp.) were used as substrates to create the microfluidic channels. A CO_2 laser from Universal

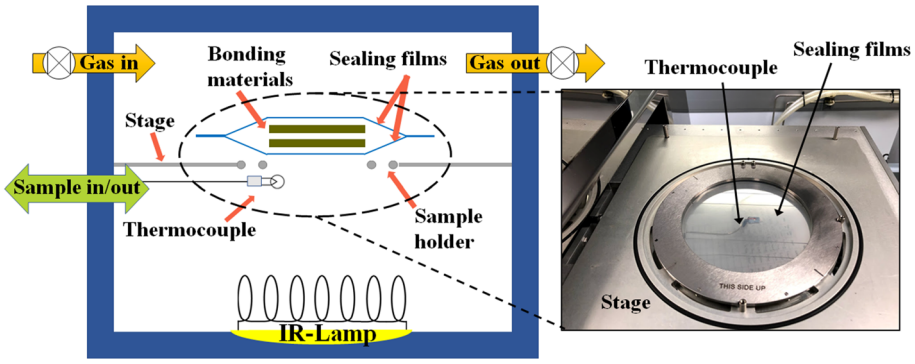

Fig. 3 Schematic of the nanoimprinter apparatus utilized for bonding polymer substrates

Laser Systems Inc. (ILS 9.75) at a power of 15 W was used in continuous wave to etch microchannels on the PMMA acrylic sheets. Acrylic pieces 4 × 6 cm^2 in size were cut along their long axis to prepare two sets of bonding specimens under the same conditions. The acrylic pieces with the etched patterns were cut in half, and each half was capped by either GATB or conventional hot pressing after 1 min of oxygen plasma treatment. The conventional hot press lamination was performed using a Carver 4388 machine equipped with a digital pressure gauge. In the conventional hot press system, thermoplastic layers were pressed between two mirror-shine polished stainless-steel sheets. In both bonding experiments, the temperature was monitored carefully by a thermocouple near the bonding components.

For cross-sectional imaging of the fluidic channels, PMMA acrylic substrates were first scored with a knife and then broken together. Measurements of microchannel dimensions were taken before and after sealing at 170 °C and 1.24 MPa for a dwell time of 1 min. Cross-section surfaces were analyzed using a Quanta FEG 450 scanning electron microscope (SEM) after conductive coating. Thickness calculations on various spots on the specimens' surface were obtained by a Mitutoyo digital micrometer before and after bonding the sheets.

3 Results and discussion

Direct bonding of thin polymer films with conventional rigid plate systems is challenging especially when the film thickness becomes small (Søndergaard et al. 2012; Gordon and Fakley 2003). Figure 4 illustrates the lamination outcome of as-received PMMA thin strip membranes bonded with two different techniques, conventional hot press and GATB. In the conventional hot press sample, contact imperfections generate a non-uniform pressure distribution that does not allow the PMMA layers to join together satisfactorily. However, on the GATB sample, the isostatic pressure accommodates surface irregularities to produce a more uniform distribution of stress. Surface imperfections, lateral shifts, and rotation between the bonded components are more easily tolerated and compensated (Gao et al. 2006). Hence, GATB can be considered as a strong candidate for joining thermoplastic surfaces to create high-strength sealed microfluidic devices. As a thermoplastic material, PMMA bonding serves as a prototype that demonstrates the concept that is applicable to a variety of thermoplastics useful for microfluidics and other applications (Mahmoodi and Besser 2018). Future work to explore the details of the GATB process with other specific thermoplastics will be of great interest for the research and manufacturing communities which can leverage this approach.

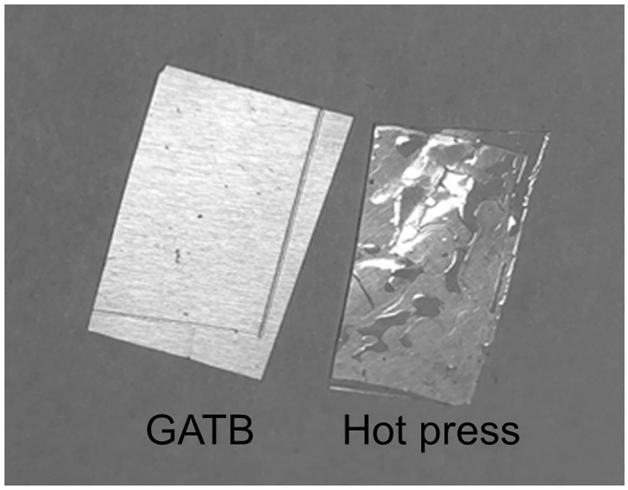

Fig. 4 Laminated PMMA membranes by GATB and conventional hot press technique at 160 °C and 1.17 MPa

3.1 Mechanical characterization

Tensile tests were carried out to study the effect of GATB processing conditions on the PMMA membranes' tensile strength. To prepare these samples, single unbonded PMMA membranes were subjected to 1.38 MPa of gas pressure at five different temperatures from 140 to 180 °C.

The product tensile strength diagram is shown in Fig. 5a. The results demonstrate a small peak at 160 °C, after which the strength slightly decreases with the further increase in the applied temperature. Accordingly, from the range of the strength recorded, it can be seen that the tensile strength of PMMA films is not remarkably influenced by the GATB treatment and the failure load after the treatment remains in the same range as for the untreated samples with a deviation of less than 2% in the average strength data.

In the next step, the cohesion between bonded PMMA films in a lap shear configuration was assessed. The lap shear test is a technique commonly used to measure the shear strength of adhesives between a wide range of combinations of similar or dissimilar materials (Gordon and Fakley 2003). The plot of the failure load versus the bonding temperature is shown in Fig. 5b. The lap shear curves at different pressures follow a similar trend with a peak appearing at 160 °C, however, the reduction in the strength after the peak happens more rapidly in the two higher pressure levels. Moreover, at GATB temperatures higher than 140 °C (and including 140 °C and 1.59 MPa), the lap shear joints were found strong enough not to allow the bonded strips to separate from their interface. Consequently, all the failures happened at the edges of the lap area except for the samples prepared at 130 °C (all three pressures) and, 140 °C at pressures of 1.17 MPa and 1.38 MPa. Also, the lap shear plots can be compared with the single membrane tensile test plots. The lap shear data shows a more pronounced peak strength at 160 °C among the other lap shear samples at different pressing temperatures. The lap shear data also shows a higher range of failure load variation with the temperature.

For samples prepared at the two lower temperatures and with which interface separation takes place, shear strength can be estimated as the measured force at breaking divided by the contact area, disregarding the nonuniform shear stress distribution and the fact that the highest shear stress happens at the overlap edges (Wu 1982). Accordingly, the average shear strength for 1.17 MPa curve rises from 0.27 to 0.29 MPa when the temperature increases from 130 to 140 °C. Comparable data has been obtained for the lap shear strength of polystyrene and poly (2,6-dimethyl 1,4-phenylene oxide) (PPO) 100-μm-thick films laminated by conventional hot pressing below T_g over relatively long time periods (Boiko and Prud'Homme 1997). The authors of the cited work recorded a shear strength of approximately 0.14 MPa for PS/PS and 0.03 MPa for PPO/PPO after bonding 24 h at respectively T_g—41 °C and T_g—126 °C (Boiko and Prud'Homme 1997). For 0.8-mm-thick COP with T_g of 136 °C, a shear strength of 0.03 MPa is reported at bonding conditions of 126 °C, 0.9 MPa, and 30 min (Pemg et al. 2010). They have shown that the bonding strength increases rapidly as bonding temperature increases, but when the bonding temperature exceeds 135 °C, the embedded microchannels start to collapse. In our work, however, the lap shear strength is studied at temperatures above T_g to analyze the high-temperature bonding conditions. A more detailed analysis of microchannel sealing at temperatures well above T_g is detailed in the next section.

The T-peel test was adopted to determine the peel strength of the joints. The T-peel test is a common approach to measure adhesion between flexible materials (Ballarin et al. 2013; Khan and Poh 2011). This method works by exerting a force perpendicular to the overlap region and by pulling the adhered materials in opposite directions to separate the contact surfaces (shown in Fig. 2). Figure 6 shows the peel strength as a function of the processing pressure. As shown, the peel strength varies only weakly with GATB pressure. Similarly, Ogilvie et al. (2010) reported that the bond pressure has little influence

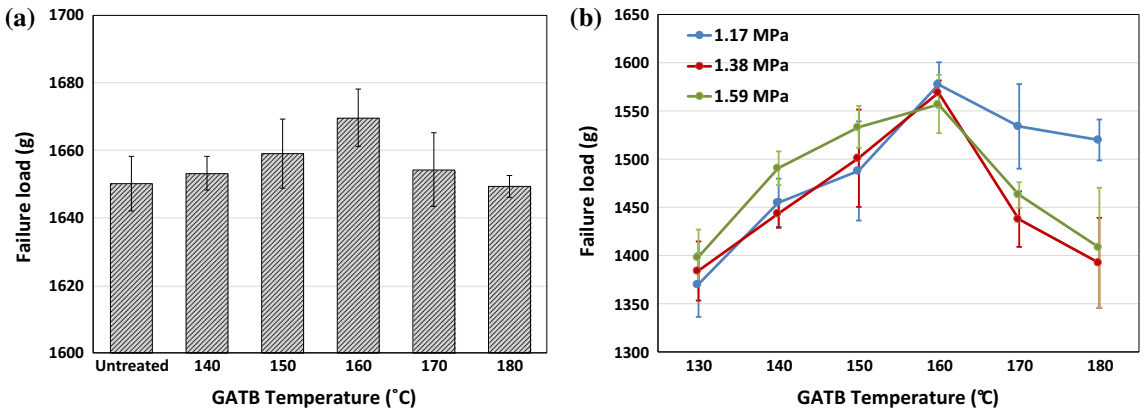

Fig. 5 **a** Recorded data for the tensile strength of unlaminated PMMA film before and after subjecting them to the GATB conditions at 1.38 MPa and different processing temperatures, **b** recorded data for the failure load with respect to the GATB processing temperature in a lap shear test. The error bars correspond to the standard deviation of the mean from at least three experiments (mean ± SD)

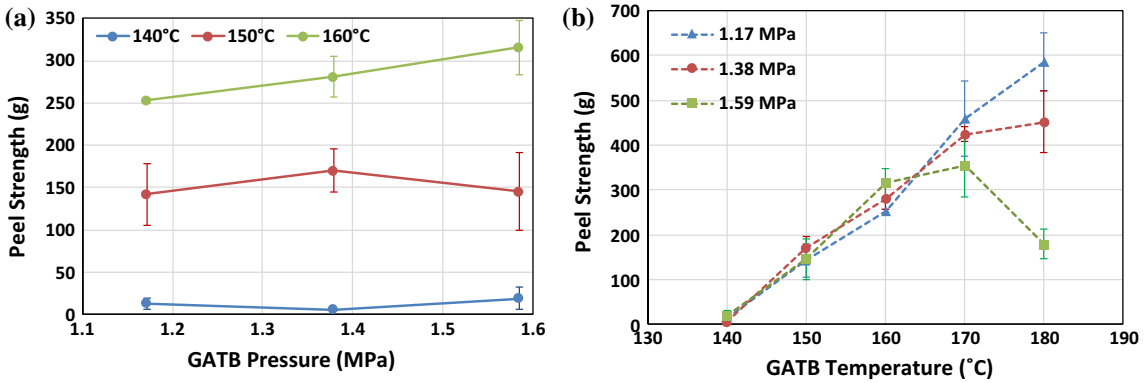

Fig. 6 **a** Recorded data for the T-peel strength vs. the GATB pressure at three different temperatures, 140 °C, 150 °C and 160 °C, **b** plot of the average peel strength against the GATB temperature at three different bonding pressure, 1.17 MPa, 1.38 MPa and 1.59 MPa. The error bars correspond to the standard deviation of the mean from at least three experiments (mean ± SD)

on the T-peel strength of PMMA acrylic sheets. However, Fig. 6a indicates that by increasing the bond temperature the overall level of the peel strength substantially improves. For the samples pressed at temperatures greater than or equal to 160 °C and pressures higher than 1.17 MPa, the peel strength becomes high enough that the overlapping area is unable to be separated through T-peel testing. Thus, we conclude that a failure mode transition in the peel strength occurs at 160 °C (Khan and Poh 2011).

Figure 6b shows the peel strength along with the GATB process temperature. The peel strength generally improves with respect to temperature. As mentioned above, at temperatures higher than 160 °C, the failure happens at the overlap edges in all samples. According to Nising et al. (2003), PMMA starts to soften at temperatures close to T_g (approximately 115 °C), however, depolymerization does not begin thoroughly until 180 °C (Becker and Gärtner 2000). Based on the results in Fig. 6b, the improved bonding strength at higher process temperatures can generally be described by the increasing numbers of bonds becoming activated to bridge the interface between the lamina. It has been reported that typically the peel strength of acrylic adhesives—chemically similar to PMMA—gradually increases with temperature, reaches a maximum, then decreases as temperature is raised further (Kim and Mizumachi 1995). This behavior agrees with the results reported here. The results of Fig. 6b are also in good agreement with the lap shear (Fig. 5b) and the single membrane tensile test results (Fig. 5a) presented earlier. While a constant increase of peel strength with temperature happens below 170 °C with all three pressures, the peel strength curves exhibit divergent behaviors based on pressure after the failure mode transition at 160 °C.

The presented mechanical results confirm that high-strength adhesive-free joining of thin thermoplastic films can be achieved using GATB. Referring to the measurements in Fig. 6b, the maximum failure load was observed for processing at 180 °C and the lower pressure of 1.17 MPa. Based on the T-peel and lap shear results, it can be concluded that when the process temperature is higher than 160 °C (the failure mode transition temperature), increasing the GATB pressure can effectively reduce the failure strength. From the tensile strength of single membranes (Fig. 5a), it was found that the decrease in the characteristic strength of the film with process temperature is relatively insignificant. It is widely agreed that high bonding pressure can induce global and localized deformation or may lead to significant thickness variation in microfluidic devices under processing conditions (Chow et al. 2005; Sun et al. 2006; Wang et al. 2011a, b). Therefore, the recorded strength results also reflect the effect of deformation on the GATB samples.

SEM cross-sections of the bonded PMMA films using GATB for 1 min at 180 °C and pressures of 1.17 MPa and 1.59 MPa are shown in Fig. 7. We observed that the overall thickness of the joined membranes stayed uniform over the entire cross-section and was measured to be about 112 µm and 106 µm for 1.17 MPa and 1.59 MPa samples, respectively. The SEM results confirm that the drop in the failure load at higher pressures can mainly be explained by the increase of deformation and thinning of the films. Increasing the processing temperature does not significantly impact the characteristic strength of the PMMA films, nevertheless this deformation is enough to drop the bonding performance of both the lap shear and T-peel specimens at temperatures above 160 °C. On the other hand, the occurrence of the peak GATB bonding strength at temperatures well above T_g indicates that GATB can effectively control the thinning of films at the applied bonding conditions. In a thermoplastic-based microfluidic system, the bonding method must not lead to deformation that results in significant dimensional change of the microchannels. For this reason, channel deformation of a

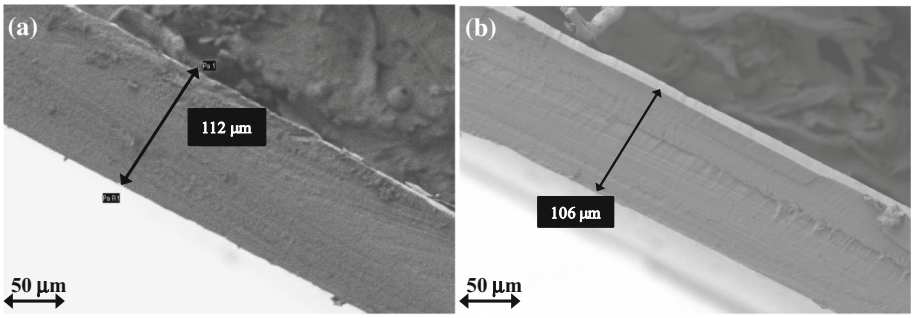

Fig. 7 SEM cross sections of GATB laminated PMMA films at 180 °C and different pressures of **a** 1.17 MPa and, **b** 1.59 MPa

PMMA-based microfluidic system after joining at elevated temperatures is studied in the next section.

3.2 Sealing of microfluidic devices

Sealing of laser-machined microchannels was compared between the GATB and conventional hot pressing (Fig. 8). To achieve this goal, PMMA acrylic sheets were first engraved by laser micromachining, and then the sheets were capped by the two different techniques. A range of sealing temperatures from 140 to 190 °C, at a constant pressure of 1.24 MPa, displayed that in a 1-min compression it is possible to seal the device at or above 150 °C, however, a robust sealing of PMMA sheets does not occur below 170 °C. This is consistent with the data achieved for the bonded PMMA membranes and a previous work on high-temperature bonding of PMMA acrylic sheets that indicates 165 °C as the required temperature (Sun et al. 2006). We observed that at temperatures lower than 170 °C, samples can easily be separated and all specimens de-bond in the cross-section preparation. When the bonding temperature is equal to or surpasses 170 °C, the bonded sheets break as a single piece. Therefore, sealing of the microchannels was performed at 170 °C to ensure a high-strength seal was achieved.

SEM cross-section images from cleaved surfaces of the pre-sealed and sealed microchannels prepared under identical bonding conditions are compared in Fig. 8b, c. The width to depth ratio (w/d) of the microchannels were collected from the SEM micrographs before and after sealing to quantitatively compare the two approaches. The results obtained from the SEM measurements are shown in Fig. 8d. The increased distortion of microchannels capped by the conventional hot press can be observed by

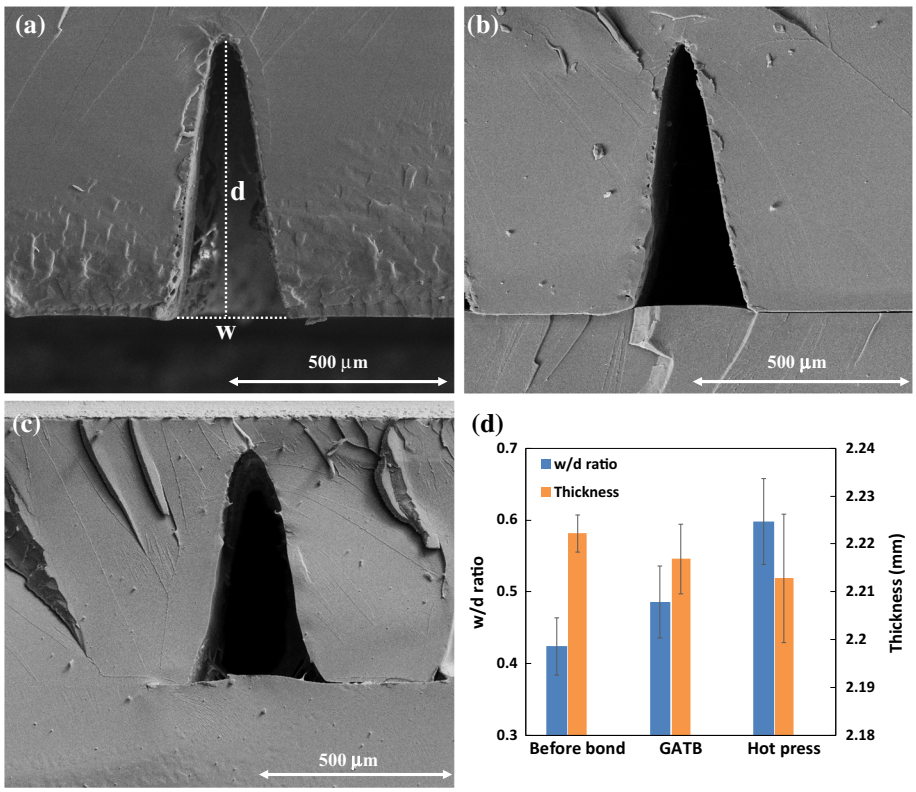

Fig. 8 Cross-section SEM images of laser micro-machined acrylic sheets, **a** before capping, **b** capping by GATB, **c** after capping by conventional hot pressing, **d** w/d ratio of microchannels and the average thickness measurements of specimens before and after bonding through the two different capping approaches. The data extracted from 10 measurements of the w/d ratio (mean ± SD, n = 10) and 10 thickness measurements per sample (5 samples) on different spots (mean ± SD, n = 50)

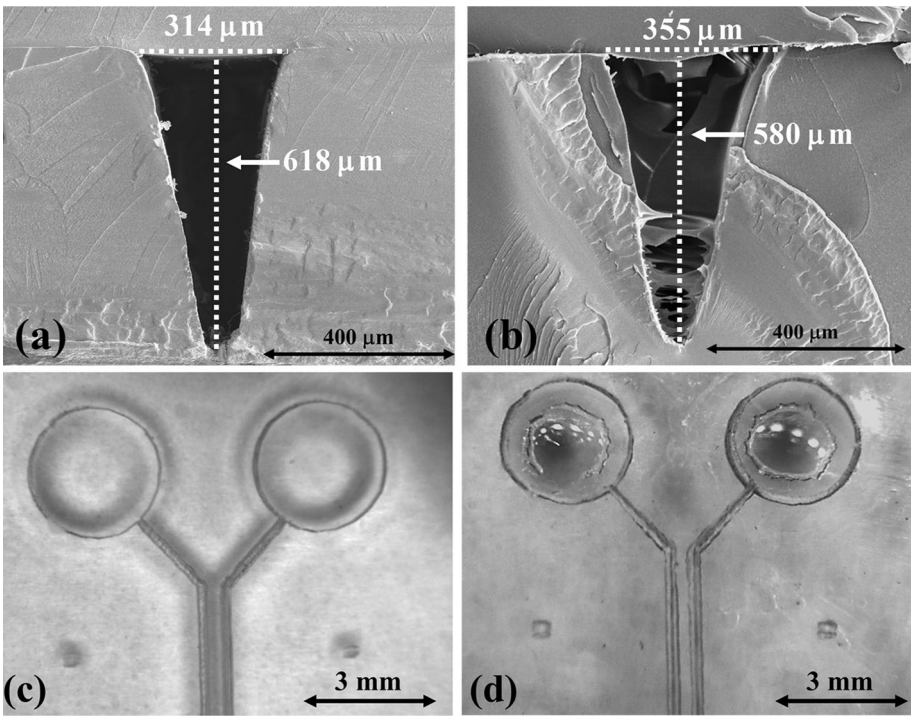

Fig. 9 Cross-section SEM images of the sealed microchannels at 180 °C and 1.24 MPa via, **a** GATB, and, **b** conventional hot pressing. Top-view of a microfluidic device sealed by **c** GATB, and **d** conventional hot pressing

comparing the w/d ratios between the two sealing approaches. Also, Fig. 8d reveals that after the sealing process, the reduction in the average thickness of PMMA sheets ($\approx 0.5\%$) is approximately $2\times$ greater for the conventional hot press samples compared to the GATB samples. Moreover, the scattering in the recorded data was found to be noticeably greater in the conventional hot press bonding, resulting in a more uniform channel shape for the GATB samples. From Fig. 8d we observe that although the substrate thinning appears to be negligible compared to the thickness of the acrylic sheets ($\sim 0.5\%$), the channel shape may be greatly affected by deformation during the sealing step.

The dimensional stability of the microchannels sealed with the two different approaches are also compared at 180 °C. Figure 9a, b show the cross-section of the sealed microchannels obtained through the two sealing methods when the bonding temperature was raised to 180 °C. The top-view of the microfluidic devices sealed at identical bonding conditions are shown in Fig. 9c, d. For both sealing conditions, the w/d ratio of the microchannels lie in the same range as observed for the 170 °C condition. Also, SEM investigations reveal that the conventional hot press-sealed specimen can experience microchannel collapse caused by uncontrolled flow of the sealing components during bonding, which can be inhibited by the GATB method (Fig. 9a).

Direct bonding of PMMA sheets at elevated temperatures has previously been reported (Sun et al. 2006; Nayak et al. 2010). Sun et al. (2006) were able to control the microchannel deformation during thermal bonding of PMMA sheets at 165 °C. They employed a relatively low pressure of 20 kPa in the hot press bonding for an extended dwell time of 2 h. Here, we have used higher bonding pressures, and the sealing was performed at 170 °C for a much shorter dwell time of one minute. Although sealing of the microfluidic devices at elevated temperatures has been avoided in most microfluidic studies to reduce the risk of deformation and unnecessary thinning of layers, the GATB technique provides the opportunity to control the microchannel deformation at elevated temperatures and consequently has potential for producing high-strength adhesive-free thermoplastic microfluidic devices.

4 Conclusion

We have described an approach for addressing existing issues with current sealing technologies of microdevices with a robust, adhesive-free and cost-effective sealing method for thermoplastic lamina. There is a significant need to resolve the challenges in MEMS packaging and fluid encapsulation in order to continue forward momentum in the field of microfluidic device technology in a variety of application areas. Existing thermal bonding approaches generally rely on a bonding temperature at or below the T_g of the material to minimize the possibility of deformation with a great investment of processing time, however, the implementation of elevated bonding temperatures (at least 50 °C above the substrate T_g) is a quicker

and more reliable route to effective sealing in thermoplastic devices.

Tensile strength results from single layer PMMA membranes reveal that applying the GATB conditions does not significantly affect the membrane's inherent strength. Lap shear and T-peel tests provided guidance toward the most suitable GATB process parameters for bonding strength. The results at different pressures and temperatures show that the failure load mostly depends on the bonding temperature and improves consistently before a distinct failure mode transition. After the transition temperature, however, higher pressures increase the risk of deformation and thinning, with potentially negative results for microdevice assembly.

We found that high-strength sealing of a microfluidic device on PMMA sheets requires a bonding temperature of at least 170 °C. When microchannel distortion at this temperature was compared between the GATB and conventional hot pressing, it was observed that GATB makes it possible to build less-distorted microchannels, with a product channel shape that is more consistent. The GATB excels in performance largely due to the isostatic pressure distribution presented to the sample surfaces during the bonding operation.

Acknowledgements The authors gratefully acknowledge the support of a fellowship provided by the Innovation and Entrepreneurship Program at Stevens Institute of Technology.

References

Ballarin FM, Blackledge TA, Davis C, Nicole L, Frontini PM, Abraham GA, Wong SC (2013) Effect of topology on the adhesive forces between electrospun polymer fibers using a T-peel test. Polym Eng Sci 53(10):2219–2227

Becker H, Gärtner C (2000) Polymer microfabrication methods for microfluidic analytical applications. Electrophoresis 21(1):12–26

Becker H, Gärtner C (2008) Polymer microfabrication technologies for microfluidic systems. Anal Bioanal Chem 390(1):89–111

Becker H, Locascio LE (2002) Polymer microfluidic devices. Talanta 56(2):267–287

Berthier E, Young EW, Beebe D (2012) Engineers are from PDMS-land, Biologists are from Polystyrenia. Lab Chip 12(7):1224–1237

Boiko YM, Prud'Homme RE (1997) Bonding at symmetric polymer/polymer interfaces below the glass transition temperature. Macromolecules 30(12):3708–3710

Brown L, Koerner T, Horton JH, Oleschuk RD (2006) Fabrication and characterization of poly(methylmethacrylate) microfluidic devices bonded using surface modifications and solvents. Lab Chip 6(1):66–73

Carlborg CF, Haraldsson T, Öberg K, Malkoch M, van der Wijngaart W (2011) Beyond PDMS: off-stoichiometry thiol–ene (OSTE) based soft lithography for rapid prototyping of microfluidic devices. Lab Chip 11(18):3136–3147

Cassano CL, Simon AJ, Liu W, Fredrickson C, Fan ZH (2015) Use of vacuum bagging for fabricating thermoplastic microfluidic devices. Lab Chip 15(1):62–66

Chen J, Zhou Y, Wang D, He F, Rotello VM, Carter KR, Watkins JJ, Nugen SR (2015) UV-nanoimprint lithography as a tool to develop flexible microfluidic devices for electrochemical detection. Lab Chip 15(14):3086–3094

Chin CD, Linder V, Sia SK (2012) Commercialization of microfluidic point-of-care diagnostic devices. Lab Chip 12(12):2118–2134

Chow WWY, Lei KF, Shi G, Li WJ, Huang Q (2005) Microfluidic channel fabrication by PDMS-interface bonding. Smart Mater Struct 15(1):S112

Eddings MA, Johnson MA, Gale BK (2008) Determining the optimal PDMS–PDMS bonding technique for microfluidic devices. J Micromech Microeng 18(5):067001

Focke M, Kosse D, Müller C, Reinecke H, Zengerle R, von Stetten F (2010) Lab-on-a-foil: microfluidics on thin and flexible films. Lab Chip 10(11):1365–1386

Folch, A. 2016. *Introduction to bioMEMS*. CRC Press

Gao H, Tan H, Zhang W, Morton K, Chou SY (2006) Air cushion press for excellent uniformity, high yield, and fast nanoimprint across a 100 mm field. Nano Lett 6(11):2438–2441

Gordon TL, Fakley ME (2003) The influence of elastic modulus on adhesion to thermoplastics and thermoset materials. Int J Adhes Adhes 23(2):95–100

Guber AE, Heckele M, Herrmann D, Muslija A, Saile V, Eichhorn L, Gietzelt T, Hoffmann W, Hauser PC, Tanyanyiwa J, Gerlach A (2004) Microfluidic lab-on-a-chip systems based on polymers—fabrication and application. Chem Eng J 101(1–3):447–453

Guo LJ (2007) Nanoimprint lithography: methods and material requirements. Adv Mater 19(4):495–513

Huang FC, Chen YF, Lee GB (2007) CE chips fabricated by injection molding and polyethylene/thermoplastic elastomer film packaging methods. Electrophoresis 28(7):1130–1137

Kelly RT, Woolley AT (2003) Thermal bonding of polymeric capillary electrophoresis microdevices in water. Anal Chem 75(8):1941–1945

Khan I, Poh BT (2011) Natural rubber-based pressure-sensitive adhesives: a review. J Polym Environ 19(3):793

Kim H, Mizumachi H (1995) Miscibility and peel strength of acrylic pressure-sensitive adhesives: acrylic copolymer–tackifier resin systems. J Appl Polym Sci 56(2):201–209

Mahmoodi SR, Besser RS (2018) Fabrication and characterization of a thin, double-sided air breathing micro fuel cell. Fuel Cells 18(4):499–508

Marasso SL, Mombello D, Cocuzza M, Casalena D, Ferrante I, Nesca A, Poiklik P, Rekker K, Aaspollu A, Ferrero S, Pirri CF (2014) A polymer lab-on-a-chip for genetic analysis using the arrayed primer extension on microarray chips. Biomed Microdevice 16(5):661–670

Matellan C, Armando E (2018) Cost-effective rapid prototyping and assembly of poly (methyl methacrylate) microfluidic devices. Sci Rep 8(1):6971

McDonald JC, Whitesides GM (2002) Poly(dimethylsiloxane) as a material for fabricating microfluidic devices. Acc Chem Res 35(7):491–499

Miserere S, Mottet G, Taniga V, Descroix S, Viovy JL, Malaquin L (2012) Fabrication of thermoplastics chips through lamination based techniques. Lab Chip 12(10):1849–1856

Nagarajan P, Yao D (2011) Uniform shell patterning using rubber-assisted hot embossing process. I. Experimental. Polym Eng Sci 51(3):592–600

Narasimhan J, Papautsky I (2003) Polymer embossing tools for rapid prototyping of plastic microfluidic devices. J Micromech Microeng 14(1):96

Nayak NC, Yue CY, Lam YC, Tan YL (2010) Thermal bonding of PMMA: effect of polymer molecular weight. Microsyst Technol 16(3):487

Nising P, Zeilmann T, Meyer T (2003) On the degradation and stabilization of poly (methyl methacrylate) in a continuous process. Chem Eng Technol 26(5):599–604

Ogilvie IRG, Sieben VJ, Floquet CFA, Zmijan R, Mowlem MC, Morgan H (2010) Reduction of surface roughness for optical quality microfluidic devices in PMMA and COC. J Micromech Microeng 20(6):065016

Park T, Song IH, Park DS, You BH, Murphy MC (2012) Thermoplastic fusion bonding using a pressure-assisted boiling point control system. Lab Chip 12(16):2799–2802

Pemg BY, Wu CW, Shen YK, Lin Y (2010) Microfluidic chip fabrication using hot embossing and thermal bonding of COP. Polym Adv Technol 21(7):457–466

Peng Linfa, Deng Yujun, Yi Peiyun, Lai Xinmin (2014) Micro hot embossing of thermoplastic polymers: a review. J Micromech Microeng 24(1):013001

Sackmann EK, Fulton AL, Beebe DJ (2014) The present and future role of microfluidics in biomedical research. Nature 507(7491):181

Søndergaard R, Hösel M, Angmo D, Larsen-Olsen TT, Krebs FC (2012) Roll-to-roll fabrication of polymer solar cells. Mater Today 15(1–2):36–49

Su YC, Shah J, Lin L (2003) Implementation and analysis of polymeric microstructure replication by micro injection molding. J Micromech Microeng 14(3):415

Sun Y, Kwok YC, Nguyen NT (2006) Low-pressure, high-temperature thermal bonding of polymeric microfluidic devices and their applications for electrophoretic separation. J Micromech Microeng 16(8):1681

Tan H, Kong L, Li M, Steere C, Koecher L (2004) Current status of nanonex nanoimprint solutions. Int Soc Opt Photon 5374:213–222

Truckenmüller R, Giselbrecht S, Rivron N, Gottwald E, Saile V, Van den Berg A, Wessling M, Van Blitterswijk C (2011) Thermoforming of film-based biomedical microdevices. Adv Mater 23(11):1311–1329

Tsao CW, DeVoe DL (2009) Bonding of thermoplastic polymer microfluidics. Microfluid Nanofluid 6(1):1–16

Tsao CW, Hromada L, Liu J, Kumar P, DeVoe DL (2007) Low temperature bonding of PMMA and COC microfluidic substrates using UV/ozone surface treatment. Lab Chip 7(4):499–505

Velten T, Ruf HH, Barrow D, Aspragathos N, Lazarou P, Jung E, Malek CK, Richter M, Kruckow J, Wackerle M (2005) Packaging of bio-MEMS: strategies, technologies, and applications. IEEE Trans Adv Packag 28(4):533–546

Wang X, Jin J, Li X, Li X, Ou Y, Tang Q, Fu S, Gao F (2011a) Low-pressure thermal bonding. Microelectron Eng 88(8):2427–2430

Wang ZY, Yue CY, Lam YC, Roy S, Jena RK (2011b) A modified quasi-creep model for assessment of deformation of topas COC substrates in the thermal bonding of microfluidic devices: experiments and modeling. J Appl Polym Sci 122(2):867–873

Wu S (1982) Polymer interface and adhesion. Marcel Dekker, New York

Zhou W (2013) Nanoimprint lithography: an enabling process for nanofabrication. Springer, Berlin

Zhu X, Liu G, Guo Y, Tian Y (2007) Study of PMMA thermal bonding. Microsyst Technol 13(3–4):403–407